Biomass and Bioenergy 213 (2026) 109383

Contents lists available at ScienceDirect

Biomass and Bioenergy

journal homepage: www.elsevier.com/locate/biombioe

Enhancement of engineered biochar functionality through co-pyrolysis of municipal wastes over metal-doped catalysts

Alireza Namdar Zangeneh [a], Maryam Abbasi [a,*], Payam Ghorbannezhad [b,c]

[a] Faculty of Civil, Water, and Environmental Engineering, Shahid Beheshti University, Tehran, Iran
[b] Institute of Catalysis Research and Technology, Karlsruhe Institute of Technology, Germany
[c] Department of Biorefinery, Faculty of New Technologies Engineering, National University of Iran, Tehran, Iran

ARTICLE INFO

Keywords:
Copyrolysis
Catalysts
Engineered biochar
Household wastes
Waste management

ABSTRACT

The escalating global waste crisis demands innovative valorization strategies. This study investigates the in-situ catalytic pyrolysis of municipal solid and food wastes to transform this stream into engineered biochar with tailored properties. Unlike prior research that primarily focuses on bio-oil upgrading, this work uniquely prioritizes biochar engineering by systematically evaluating three distinct catalyst families—HZSM-5 (Brønsted acid), Na-ZSM-5 (basic/neutral), and Fe_3O_4 (redox-active)—and their modification with nickel or cobalt (5 wt%). Pyrolysis at 550 °C was selected based on thermogravimetric analysis to optimize the trade-off between biochar yield and carbonization degree. HZSM-5-based catalysts maximized biochar yield (40.9%), while Fe_3O_4-based catalysts favored bio-oil and biogas production. Metal coating generally reduced bio-oil yield, promoting non-condensable gas formation. Critically, catalyst selection and coating dictated biochar properties. Base catalysts, particularly Fe_3O_4, produced biochar with high specific surface areas (up to 480 m^2/g). However, metal coating introduced catalyst particles onto the biochar surface, observed via FESEM/EDX, which reduced this area but significantly enhanced thermal stability (as low as ~15% weight loss by TGA). These findings demonstrate that catalytic pyrolysis can strategically tailor biochar, creating composites with active sites and robust stability. This positions waste-derived biochar as a promising, sustainable material for advanced applications, including catalysis and energy storage, particularly after post-processing to reclaim surface area.

1. Introduction

Economic growth and urbanization have led to increased consumption, resulting in a rise in the generation of municipal solid waste (MSW) [1]. According to the World Bank projections, worldwide municipal waste is expected to reach 3.4 billion tons annually by 2050 [2]. Also, the World Bank reported in 2018 that the average generation of municipal waste per capita in Iran was 650 g per day, approximately equivalent to the Middle East and global averages [2]. However, Iran ranks poorly in waste management practices among other countries [2]. Despite accounting for nearly 70% of Iran's municipal solid waste, exceeding both regional and global averages, organic materials are poorly managed. These materials present a valuable opportunity for resource recovery through composting, energy production, or the generation of other beneficial byproducts via various processes. However, over 70% of Iran's municipal waste is still disposed of through practices like open dumping or landfills that fail to meet proper standards. Moreover, improper waste management practices, including unsanitary disposal methods, can lead to air pollution through greenhouse gas emissions and contamination of soil and water resources through leachate generation, posing severe environmental and health challenges [3].

Various methods exist for municipal waste disposal. Landfills, which can contain large amounts of municipal waste, are widely used in many countries [4]. However, landfills occupy extensive areas, and landfill leachate may contaminate soil and groundwater, while gases emitted from waste can pollute the air [4,5]. On the other hand, incineration can reduce the volume of municipal waste through thermal processing, and compared to landfills, incineration requires less land area, and the heat generated from the process can be utilized for electricity generation and heating systems. However, the emission of particulate matter, fly ash, and pollutants such as dioxins NO_x and SO_2 from incineration can harm the environment [6]. Fast pyrolysis is considered an effective,

This article is part of a special issue entitled: Biochar IV published in Biomass and Bioenergy.

* Corresponding author.
E-mail address: payam.ghorbannezhad@partner.kit.edu (M. Abbasi).

https://doi.org/10.1016/j.biombioe.2026.109383
Received 6 October 2025; Received in revised form 2 April 2026; Accepted 2 April 2026
Available online 6 April 2026

List of abbreviations

HZ	HZSM-5
Ni/HZ	Ni/HZSM-5
Co/HZ	Co/HZSM-5
NaZ	Na-ZSM-5
Ni/NaZ	Ni/Na-ZSM-5
Co/NaZ	Co/Na-ZSM-5
Fe	Fe3O4
Ni/Fe	Ni/Fe3O4
Co/Fe	Co/Fe3O4

cost-effective, and environmentally friendly method for processing MSW and biomass, producing value-added products such as bio-oil and biochar [7,8]. Biochar produced from pyrolysis, despite its limitations, can have significant environmental applications such as mitigating climate change, reducing greenhouse gas emissions, especially carbon dioxide, water purification, soil improvement, energy storage, and catalysis, depending on its characteristics [9,10].

Despite extensive research on catalytic pyrolysis, a critical knowledge gap remains: most studies prioritize bio-oil yield and quality, often treating biochar as a low-value byproduct [11–14]. Consequently, the systematic influence of different catalyst families—particularly comparing acidic zeolites (HZSM-5), basic/neutral zeolites (Na-ZSM-5), and redox-active metal oxides (Fe_3O_4)—on the physicochemical properties of biochar remains underexplored. Furthermore, while transition metal modification (e.g., Ni, Co) is commonly employed to enhance catalytic activity for bio-oil production, its specific impact on biochar surface chemistry, porosity, and thermal stability has not been systematically investigated. This study addresses this gap by shifting the focus from bio-oil to biochar engineering, providing a comprehensive evaluation of how catalyst type and metal coating dictate biochar properties for targeted applications.

Several approaches have been investigated to improve the production and the quality of pyrolysis products, such as co-pyrolysis of different types of waste with various compositions [15–17], conducting the process at different temperatures [18,19] and under different atmospheres [20–22], with various feeding rates [18,23], using catalysts [24–26], and other parameters. Among these approaches, using catalysts has been widely popular and studied to enhance the yield and quality of fast pyrolysis products. However, in most studies on catalytic pyrolysis of waste, less attention has been paid to changes and improvements in biochar properties, as the main focus has been on increasing the production and quality of bio-oil or gas [11–14]. This gap is significant because biochar, if properly engineered, can serve as a sustainable material for catalysis, energy storage, and environmental remediation, potentially offering higher economic value than bio-oil in certain contexts.

Research focusing on biochar derived from biomass pyrolysis has predominantly mentioned waste composition as the primary determinant of biochar quality, and/or cited the effect of catalysts on biochar's quality as negligible. Leng et al. showed that the presence of alkaline and alkaline earth metals in biomass can act as self-activators for pore development during pyrolysis [27]. In the study conducted by Ghorbannezhad et al., the horticultural-to-municipal wastes ratio in catalytic co-pyrolysis was stated as the primary factor determining the yield of biochar, with the highest production achieved without the use of zeolite catalyst [5]. The work of Raček et al. on catalytic pyrolysis of food waste using zeolite and metal oxide as catalysts demonstrated the effect of the initial waste composition on the properties of the produced biochar, also noting the insignificant changes in BET surface area and calorific value of it, despite the use of catalysts [28].

However, these studies either employed a single catalyst type or did not systematically vary catalyst chemistry to understand its role in biochar formation. Moreover, the use of metal coatings (Ni, Co) on distinct catalyst supports to tailor biochar properties has not been comparatively evaluated. Therefore, this study moves beyond a descriptive comparison of catalyst types by providing a mechanistic insight into how catalyst acidity, basicity, and redox properties influence biochar yield, porosity, surface chemistry, and thermal stability.

The novelty of this work lies in three key aspects: (1) systematic comparison of three fundamentally different catalyst families (acidic zeolite, basic/neutral zeolite, and metal oxide) under identical pyrolysis conditions; (2) evaluation of Ni and Co modification on each catalyst specifically for biochar engineering rather than bio-oil upgrading; and (3) comprehensive characterization linking catalyst properties to biochar functionality, including BET surface area, thermal stability (TGA), surface morphology (FESEM), and elemental composition (EDX). This integrated approach provides a roadmap for selecting catalyst systems to produce application-specific biochars, addressing a critical need in waste valorization.

Therefore, this study aims to investigate the impact of three base catalysts (HZSM-5, Na-ZSM-5, Fe_3O_4) and transition metals used to coat them (nickel and cobalt separately), resulting in a total of nine distinct catalysts on the production and quality of biochar derived from municipal waste pyrolysis through the analysis of its physical, chemical, and physicochemical properties, which determine its future applications.

2. Materials and methods

2.1. Feedstock preparation and characterization

The municipal waste used in this experiment was typical garbage (household waste) collected from Tehran, Iran. This sample represented an intricate medley of recoverable materials alongside biodegradable substances, constituting the bulk (roughly 70%) of Tehran's waste stream [29]. These biodegradable components include wood and paper, along with other organic constituents (such as fruit and vegetable wastes). Upon disposal at landfill sites, recyclable materials are separated, leaving predominantly biodegradable waste. The waste sample was also heterogeneous to a great degree in terms of its material composition, regardless of its geometry or particle size. A fraction of the original sample with particle sizes less than 1 mm was obtained by mechanically shredding the waste samples in a grinder. This was followed by sieving after air-drying at room temperature for 24 h. Subsequently, the waste samples underwent uniform mixing for 2 h using a micro rotary mixer. Carbon, hydrogen, nitrogen, and sulfur fractions were determined using the EuroEA3000 elemental analyzer and the 5E-AS3200B automatic Coulomb sulfur analyzer, respectively. The ultimate analysis was performed using a thermogravimetric analyzer (NETZSCH, TG-209-F3), and the final analysis was conducted using Thermo Fisher's Flash 2000 elemental analyzer. Levels of ash and oxygen were determined using a mass equilibrium approach. The properties of the feedstock were determined through the ultimate and proximate analyses of municipal waste conducted on a dry basis. All experiments were performed twice for data validation and to ensure the replicability of the results.

2.2. Catalysts preparation

The three base catalysts used in this study were HZSM-5, Fe_3O_4, and Na-ZSM-5, which is formed during the production process of ZSM-5 and is the sodium form of this catalyst, were all procured from Bakhtar group company in Tehran, Iran. HZSM-5 was selected for its strong Brønsted acidity, Na-ZSM-5 for its neutral/basic properties with reduced acidity, and Fe_3O_4 for its redox activity and magnetic separability.

A 5 wt% loading of Ni and Co was selected based on preliminary screening and literature reports indicating that this loading provides a

balance between catalytic activity and metal dispersion without excessive coke formation [30,31]. The surface of a fraction of these fine-grained base catalysts (particle size range of 0.025–0.106 mm) was coated with nickel, while the surface of another portion was coated with cobalt separately. Salt forms of these two metals as hexahydrate nickel nitrate and hexahydrate cobalt nitrate produced by MERCK were procured and used to prepare the coated catalysts. Nickel and cobalt were chosen as transition metals as they promote secondary reactions (dehydrogenation, deoxygenation) during the process while being more accessible and economical compared to noble transition metals. This resulted in a total of nine distinct catalysts for this study (3 base catalysts, three nickel-coated base catalysts, and three cobalt-coated base catalysts).

In this study, each of the three base catalysts was coated with an amount of nickel and cobalt equal to 5% of their weight (e.g., Ni/HZSM-5 = 5 g Ni + 100 g HZSM-5). The catalyst coating process was carried out using the wet impregnation method, which involved bringing the catalyst and metal salt into contact in an aqueous environment. Therefore, the catalysts were dispersed in an appropriate amount of water in a laboratory glass container to achieve low concentration and placed on a magnetic stirrer. The speed of the device was adjusted so that mixing would occur well to ensure uniform catalyst concentration throughout the solution. Next, the metal salt, dissolved in 30 mL of water, was gradually added to the laboratory flask using a 50 mL burette emptied after 25 min, allowing the metal to mix with the water-catalyst solution adequately. The magnetic stirrer continued mixing the solution for another 3 h after emptying the burette to ensure complete mixing of the catalyst and metal. Subsequently, the laboratory glass container was placed in an oven at 80 °C for 24 h for the coated catalyst to dry. The remaining powder was then subjected to 300 °C in an oven for 3 h to eliminate any organic matter that might have entered the powder during the process. While this method ensures metal deposition, further characterization (e.g., XPS, TEM) would be required to confirm the homogeneity and stability of metal dispersion, which is acknowledged as a limitation of this study.

2.3. Experimental setup

To investigate the influence of base catalysts and their respective metal coatings (nickel and cobalt) on the yield and quality of biochar, other parameters were kept constant throughout the experiments, including reactor's temperature (550 °C; this temperature was selected based on preliminary TGA results showing maximum volatile matter release from the feedstock, and consistent with literature indicating that 500–600 °C is optimal for balancing biochar yield and carbonization degree in municipal waste pyrolysis), feedstock residence time (1 min), waste-to-catalyst ratio (27g waste to 3g catalyst), and the flow rate of nitrogen gas (200 mL/min) as the carrier gas in the system. The only variable parameter was the catalyst employed.

The experimental setup, as depicted in Fig. 1, employed a screw feeder to deliver a consistent mass of 30 g of feedstock into the pyrolytic reactor for each experiment. Two asbestos plungers functioned as thermal insulators, separating the feedstock boat from the temperature zone. To prevent premature combustion of the feedstock and clogging at the screw feeder exit, circulated water was continuously pumped around the feedstock boat. The central component of the setup consisted of a fixed-bed reactor. The reactor was cylindrical in shape, having a diameter of 1.5 inches (3.18 cm) and constructed from steel. Quartz insulation enveloped the reactor to minimize heat loss. A programmable heater with a precisely controlled heating rate and residence time provided the necessary thermal conditions within the pyrolytic reactor. The vaporized products, including pyrolysis gas, were cooled and collected in a condensed section composed of a condenser and a heat exchanger. The residual pyrolytic biochar was retrieved from the system, weighed to determine the yield distribution, and further analyzed to characterize its properties. Each experiment was repeated twice, and product yields

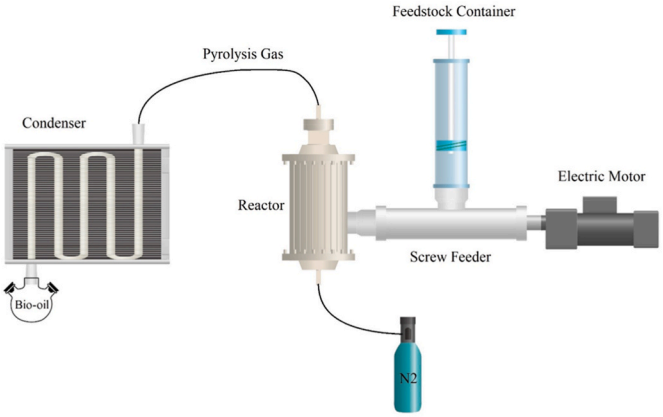

Fig. 1. Schemcatic of experimental set-up.

are reported as average values with standard deviations to account for feedstock heterogeneity and experimental variability.

2.4. Product evaluation

For biochar, properties such as its physical characteristics like specific surface area and porosity, as well as its thermal stability and constituent elements, are of importance. Thermogravimetric analysis was conducted using a TGA Q5000 thermogravimetric analyzer (TA Instruments, New Castle, USA) to determine the thermal behavior of biochar samples. The samples were heated in the range of 30 to 800 °C at a rate of 20 °C per minute, with nitrogen gas flowing at a rate of 60 mL/min as the carrier gas. Surface morphology and microstructure of biochar particles were examined using field emission scanning electron microscopy (in the range of magnification from 50 μm to 500 nm), and energy-dispersive X-ray spectroscopy was conducted to determine the constituent elements of biochar (carbon, oxygen, nitrogen, calcium, iron, nickel, potassium, sodium, zinc, copper, and chromium), both using MIRA3 FEG-SEM (TESCAN, Brno, Czech Republic). BET analysis was also conducted to determine the specific surface area of the sample particles based on ASTM D4641-12 using nitrogen adsorptive gas, and the BET surface area was determined using the BET equation.

3. Results and discussion

3.1. Characterization of feedstocks

The results of the proximate and ultimate analyses of the feedstock are presented in Table 1. The composition of the feedstock holds significant importance as it plays a vital role in the quantity, quality, and characteristics of the biochar produced from pyrolysis [32]. For instance, the presence of higher amounts of carbon and oxygen in the feedstock (like the feedstock of this study) can lead to increased biochar production [33]. Volatile matter, present in considerable amounts in the present sample, primarily constitutes the gas conversion during pyrolysis, which can possibly be condensed and transformed into bio-oil [34]. The process temperature highly influences this transformation of volatile matter to gas and the quantity of biochar and bio-oil produced [34].

On the other hand, the amounts of fixed carbon and ash, which play a determining role in the quantity and quality of biochar, depend more on the initial composition of the feedstock [35]. Fixed carbon consists of resilient and highly aromatic carbon that is resistant to decomposition at high temperatures, thus not easily transformed into gas and, subsequently, bio-oil. The ash content also decreases slightly due to its inorganic nature during the process temperature and provides a measure of the relative inorganic compounds in the sample [36]. Among these compounds, volatile matter and ash content are of significant importance for biochar intended for use as soil amendment [34]. Similarly, the

Table 1
Physiochemical properties of feedstocks and Biochar.

Component	Municipal Waste	Food Waste	Biochar
Proximate Analysis (wt%, ar*)			
Moisture	9.3 ± 0.47 (5.1%)	5.1 ± 0.26 (5.1%)	4.3 ± 0.22 (5.1%)
Volatile	77.2 ± 2.32 (3.0%)	87.3 ± 2.62 (3.0%)	49.3 ± 1.48 (3.0%)
Fixed carbon	10.1 ± 0.40 (4.0%)	5.4 ± 0.22 (4.1%)	36.2 ± 1.45 (4.0%)
Ash	3.4 ± 0.14 (4.1%)	2.2 ± 0.09 (4.1%)	10.2 ± 0.41 (4.0%)
Ultimate Analysis (wt%, db*)			
C	42.1 ± 1.26 (3.0%)	39.8 ± 1.19 (3.0%)	65.3 ± 1.96 (3.0%)
H	6.4 ± 0.19 (3.0%)	6.7 ± 0.20 (3.0%)	4.3 ± 0.13 (3.0%)
N	0.5 ± 0.04 (8.0%)	1.1 ± 0.09 (8.2%)	3.01 ± 0.24 (8.0%)
S	0.8 ± 0.06 (7.5%)	0.6 ± 0.05 (8.3%)	0
O	50.2 ± 1.51 (3.0%)	51.8 ± 1.55 (3.0%)	27.4 ± 0.82 (3.0%)
Metal content (ppm, db*)			
Ca	10342 ± 724 (7.0%)	103 ± 7.2 (7.0%)	9104 ± 637 (7.0%)
Fe	1196 ± 84 (7.0%)	97 ± 6.8 (7.0%)	586 ± 41 (7.0%)
Mg	1584 ± 111 (7.0%)	108 ± 7.6 (7.0%)	936 ± 66 (7.0%)
Na	438 ± 31 (7.1%)	99 ± 6.9 (7.0%)	435 ± 30 (6.9%)
P	352 ± 25 (7.1%)	81 ± 5.7 (7.0%)	123 ± 8.6 (7.0%)
Al	1377 ± 96 (7.0%)	56 ± 3.9 (7.0%)	97 ± 6.8 (7.0%)
K	1201 ± 84 (7.0%)	118 ± 8.3 (7.0%)	1017 ± 71 (7.0%)
Ti	35 ± 3.5 (10.0%)	-	-
Zn	41 ± 4.1 (10.0%)	1 ± 0.1 (10.0%)	-
BET Analysis (m^2/g)			
	-	-	6.7 ± 0.47 (7.0%)

nitrogen content present in biochar plays a vital role in its performance as a fertilizer. The presence of macromolecular amino acids and proteins in the feedstock, prevalent in household waste containing fruit peels, and confirmed by the results of the final analysis of the feedstock of this study, contributes to the high nitrogen content in biochar [34]. The high ash content, unlike volatile matter which, upon evaporation, often leads to the formation of pores and micropores, results in pore clogging and reduction in the surface area of micropores, subsequently limiting the adsorption sites on the biochar surface, making it undesirable for adsorption-related applications [27]. Conversely, the presence of alkali and alkaline earth metals in the feedstock can promote the development of biochar pores due to their self-activating ability [27]. Also, lower moisture content is also desirable due to reduced energy required for the pyrolysis process and easier storage and transportation of waste because of significant volume reduction [34].

3.2. Pyrolysis product distribution

The distribution of pyrolysis products for each of the nine catalysts is shown in Fig. 2. Among the three base catalysts, HZSM-5-based catalysts exhibited the highest average biochar yield of 40.9% wt. of feedstock, with the highest individual biochar yield of 42.2% wt. achieved in the experiment with HZSM-5. On the other hand, Fe_3O_4-based catalysts demonstrated the highest average bio-oil yield of 32.3% wt., with the highest individual bio-oil yield of 35.2% wt. obtained in the experiment using Fe_3O_4 as the catalyst. This observation can be explained by the distinct catalytic mechanisms of zeolite-based catalysts versus metal oxides. Zeolites (HZSM-5 and Na-ZSM-5) possess Brønsted and Lewis acid sites that promote cracking, dehydration, and decarboxylation reactions, which typically reduce bio-oil yield but improve its quality [37]. The higher bio-oil yield observed with Fe_3O_4 can be attributed to its redox properties, which favor the formation of oxygenated intermediates that remain in the condensable fraction, as well as its lower acidity compared to zeolites, reducing the extent of secondary cracking to non-condensable gases.

Na-ZSM-5-based catalysts, on the other hand, exhibited the lowest average biochar yield of 36% wt. and the highest average biogas yield of 40.7% wt. The highest biogas yield of 43.2% wt. was achieved in the experiment with Ni/NaZSM-5. The lower biochar yield of these catalysts can be attributed to the reduced coke formation on biochar due to the presence of sodium, which enhances gasification reactions and limits carbonaceous residue accumulation [38].

Additionally, the higher biogas production can be explained by the presence of sodium as a coke reducer on the catalyst, preventing catalyst deactivation. The higher biochar yield of HZSM-5-based catalysts may be due to their more significant potential for coke formation and catalyst deactivation, as well as increased biochar production due to contact with metals like potassium, which were later detected in the biochar composition [39]. The results of the BET analysis also indicate a lesser decrease in the biochar surface area of these catalyst samples compared to those of other catalysts.

Comparing the product yields of uncoated base catalysts to nickel- and cobalt-coated catalysts reveals a decrease in bio-oil production for all three catalysts after coating. This can be attributed to differences in catalyst surface areas. Dzol et al. demonstrated that the BET surface area of the Ni-WCE/HZSM-5 catalyst decreased due to nickel impregnation [31]. Similarly, Miskolczi et al. reported in their study that the introduction of additional transition metals to the catalyst surface reduced their specific surface area [30]. Since the rate of thermal decomposition reactions is primarily dependent on the catalyst's specific surface area, a larger surface area leads to a higher degree of pyrolysis reactions [30]. Furthermore, it is observed that all nickel-coated catalysts exhibited the highest biogas production for each base catalyst. This can be attributed to nickel's ability to promote deoxygenation, dehydrogenation, and decarbonylation of compounds, which is another reason for the reduced bio-oil yield of coated catalysts, as these mechanisms lead to the

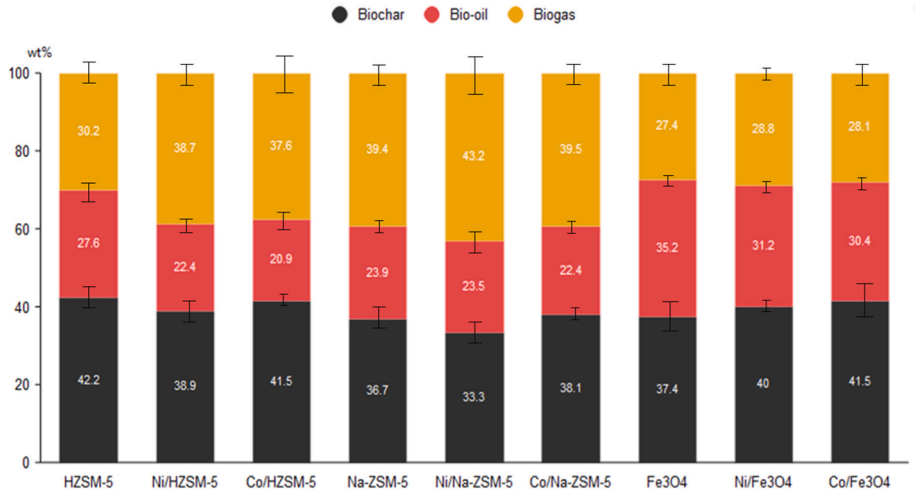

Fig. 2. Distribution of yield pyrolysis products for each catalyst.

formation of non-condensable gases [40]. It should be noted that the gas composition (e.g., H_2, CO, CH_4, CO_2) was not analyzed in this study, which limits the mechanistic understanding of these secondary reactions. This is acknowledged as a limitation, and future work will include gas chromatography analysis to quantify product gas speciation.

3.3. BET surface

BET analysis was conducted on all samples to assess the specific surface area and porosity of the biochar samples. The results for the BET specific surface area of the biochar samples are presented in Table 2. Typically, the specific surface area of biochar falls within the range of 8 to 132 m^2/g [27]. Uncoated catalysts exhibited higher specific surface areas. However, Na-ZSM-5-coated biochar samples displayed a lesser decrease in surface area compared to other coated catalyst samples.

The presence of catalysts on the biochar's surface and their catalytic activity leads to increased evaporation of volatile matter [27]. Nonetheless, the concentration of organic volatiles, particularly considering the high volatile content of the feedstock, may block pores after pyrolysis [41]. It is noteworthy that nickel-coated catalysts exhibited a more significant decrease in specific surface area and lower BET specific surface areas compared to cobalt-coated catalysts, which may be due to the higher dehydrogenation and deoxygenation ability of nickel [40]. These reactions can contribute to increasing the carbon content of the biochar by promoting the evaporation of hydrogen and oxygen, thereby densifying the biochar's structure. This increased densification of the biochar's structure may subsequently lead to a reduction in the BET surface area of the biochar by closing smaller pores, especially micropores [27,42]. Despite differences in the extent of their abilities to promote these reactions, both nickel and cobalt catalysts enhance such reactions. Consequently, all coated catalysts exhibited lower BET surface areas compared to their uncoated counterparts. The exceptionally high surface area of the Fe_3O_4-derived biochar (480.3 m^2/g) is noteworthy. This value significantly exceeds typical ranges for biochar produced from municipal waste and can be attributed to a synergistic effect: (1) the self-activating role of alkali and alkaline earth metals inherently present in the feedstock, which promote pore development during pyrolysis [27], and (2) the catalytic activity of Fe_3O_4, which may enhance the release of volatile matter and create additional porosity. This finding suggests that Fe_3O_4 is particularly effective for producing high-surface-area biochar without post-treatment activation.

The more substantial decrease in specific surface area for Fe_3O_4-based samples may be attributable to its lower surface area and well-defined, in comparison to zeolite-based catalysts, which provide abundant active sites for catalytic reactions and adsorption processes [25,39]. Furthermore, the formation of coke on the samples because of secondary catalytic reactions leads to further pore blockage [43,44]. The lesser decrease in surface area for Na-ZSM-5-based samples can be explained by the reduced coke formation by these catalysts due to the presence of sodium [31].

3.4. FESEM analysis

FESEM analysis was performed on two biochar samples, Fe and Ni/Fe. Biochar samples exhibit complex morphology due to the feedstock's complex composition. The surface morphology of the Fe sample is shown in Fig. 3. These images reveal a porous structure with irregularly shaped particles. Kumar et al. achieved similar results for biochar derived from apple peel pyrolysis, attributing the formation of deep porous channels to the extensive removal of volatile organic matter during pyrolysis [45]. Other studies have also suggested that the release of volatile matter in the form of small molecules (H2O, CO, CO2, CH4, etc.) during the thermal conversion process of biomass in pyrolysis leads to the creation of these pores on the biochar surface [46,47]. It is also observed that the size and shape of particles and pores are relatively similar. Another important observation from the higher magnification images is the deposition of iron catalyst particles on the biochar (some marked with red arrows). The deposition of the catalyst on the biochar creates active sites that are influential in both the pyrolysis process and secondary mechanisms and are highly significant for future applications of biochar as a catalyst or energy storage material [40,48,49]. It can be seen that iron particles are deposited inside the pores, indicating the presence of active sites within the pores as well (see Fig. 4).

Fig. 3 presents images of the Ni/Fe biochar sample. These images also show a similar texture and particle size as before. The main difference, which was also apparent in the BET analysis results, is the reduced porosity. As mentioned, this may be attributed to the densification of the biochar's structure and the increase in carbon content, especially when using coated catalysts. It is also evident that catalyst particles are present within the biochar pores. As mentioned, all these particles are active sites and also lead to an increase in the sample's acidity. Thus, the same applications mentioned for the Fe sample are also valid for this sample, and this sample may even be more suitable for the applications described above due to the presence of more sites due to the addition of nickel. However, this sample will require more post-treatment due to the reduced surface area and porosity.

3.5. EDX analysis

The elemental composition of Fe and Ni/Fe biochar samples is presented in Table 3. The results revealed an increase in carbon content compared to the original municipal waste (household) feedstock. This is attributed to the dehydration, cracking, and polymerization reactions that occur during pyrolysis, leading to the reconstruction of decomposable carbon compounds, while other elements may be lost through volatilization [50,51]. The decrease in oxygen and increase in carbon indicate the successful pyrolysis process. Moreover, the presence of various elements such as N, K, Na, Ca, Fe, Zn, Cu, and Cr in the biochar, which are essential nutrients for soil fertility and crop productivity enhancement [51], makes these biochar suitable candidates for use as fertilizers and soil amendments.

A significant observation from the EDX analysis is the presence of iron in both Fe and Ni/Fe samples at 39.0 and 47.0 wt%, respectively, and the presence of nickel in the Ni/Fe sample at a notable concentration of 48.6 wt%. This confirms the significant deposition of catalyst metals onto the biochar's surface, particularly in the Ni/Fe sample with its high nickel content, which aligns with the observations from FESEM images and BET analysis. The presence of these metals, due to their ability to facilitate high ion exchange and potentially abundant acidic sites, makes these biochars promising candidates for catalytic applications [52]. Additionally, with appropriate post-treatment, these biochars could be utilized as electrodes and energy storage materials [9]. However, direct experimental evidence of catalytic activity or electrochemical performance was not obtained in this study; therefore, these proposed applications remain speculative and will be the focus of future work.

3.6. Proposed reaction pathways for metal-modified catalysts in biochar formation

Based on the experimental observations—including product yield

Table 2
BET surface area of each biochar sample.

Sample	HZ	Ni/HZ	Co/HZ	NaZ	Ni/NaZ	Co/NaZ	Fe	Ni/Fe	Co/Fe
S_{bet} (m^2/g)	117.114	17.1	18.344	105.081	47.345	56.506	480.337	13.155	17.446

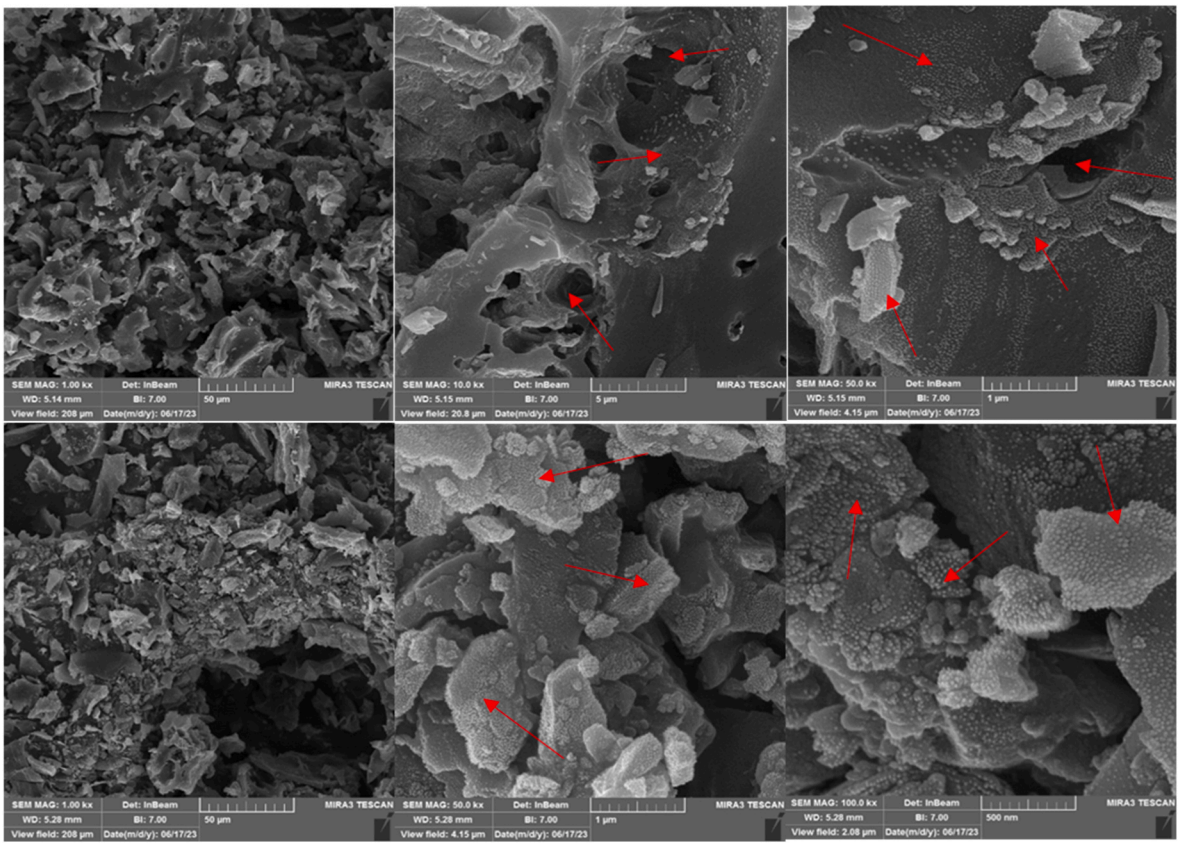

Fig. 3. Morphological analysis by FESEM, Fe (above), Ni/Fe (below).

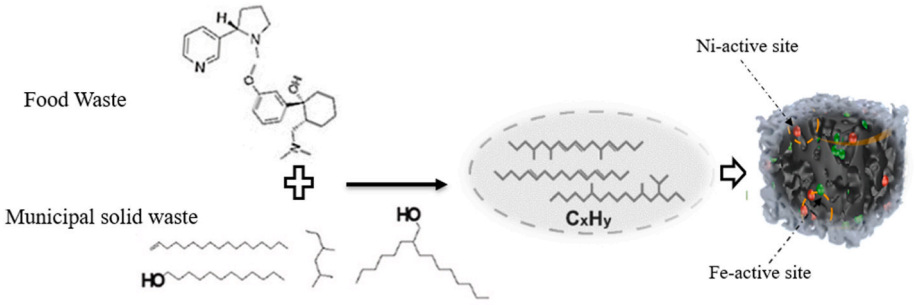

Fig. 4. Mechanism of Ni and Fe doped Biochar during co-pyrolysis.

Table 3
Constituent elements of Fe and Ni/Fe.

Sample	Fe	SD (%)	Ni/Fe	SD (%)
Element (wt%)				
C	65.13	±3.91 (6%)	68.53	±4.11 (6%)
O	20.50	±1.23 (6 %)	15.96	±0.96 (6%)
N	3.07	±0.28 (9.1%)	2.67	±0.24 (9%)
Na	2.18	±0.2 (9%)	2.56	0.23 (9%)
Ni	–		4.24	
K	1.56	±0.14 (9%)	1.32	±0.12 (9%)
Ca	1.42	±0.13 (9%)	1.16	±0.10 (9%)
Fe	4.47	±0.4 (9%)	2.35	±0.21 (9%)
Cu	1.05	±0.10 (9.5 %)	0.89	±0.09 (10%)
Cr	0.46	±0.05 (11%)	0.23	±0.03 (13%)
Zn	0.16	±0.02 (12.5%)	0.09	±0.01 (11)

distributions, BET surface area trends, and FESEM/EDX confirmation of metal deposition—a plausible reaction pathway is proposed. During the catalytic pyrolysis stage, the feedstock undergoes thermal degradation into long-chain radical intermediates via random scission of C–C bonds. The oxygenated functional groups and the developing porous structure of the biochar matrix may attract these volatile intermediates, where heterogeneous catalytic reforming and cracking occur. The doping of Ni and Fe particles enhances the availability of Lewis acid sites, which are hypothesized to facilitate deoxygenation, dehydrogenation, and cracking reactions. Consequently, radical fragments may undergo hydrogen transfer, converting into straight-chain hydrocarbons (e.g., light alkenes and alkanes) in the bio-oil fraction. These alkenes may subsequently undergo aromatization and oligomerization, contributing to aromatic hydrocarbon formation. While this proposed pathway is consistent with the observed reduction in bio-oil yield and increase in biogas production with metal-coated catalysts, it remains speculative. Direct evidence—such as in-situ DRIFTS, gas composition analysis (H_2, CO, CH_4, CO_2), and detailed kinetic modeling—is required for validation and is recommended for future studies.

This study demonstrates that the co-pyrolysis-catalysis of municipal

and food waste using metal-doped catalysts yields distinct product distributions and biochar properties compared to non-catalytic or single-catalyst systems. Overall, the research validates the feasibility of converting municipal and food waste into value-added biochar and hydrocarbons through a catalytic pyrolysis process.

3.7. Thermogravimetric analysis

The thermal stability of Fe, Ni/Fe, and HZ biochars was investigated using a TGA/DTG analyzer. The TGA and the DTG curves for Fe, Ni/Fe, and HZ biochars are presented in Fig. 5. The initial weight loss peak for all samples occurred in the range of 30-100 °C, attributed to the evaporation of absorbed moisture. The weight losses for Fe, Ni/Fe, and HZ were 1.0%, 1.5%, and 1.5%, respectively. The weight loss trends of Fe and Ni/Fe biochars suggests similar thermal resistance. In the range of 200-550 °C, the DTG curves show more weight changes for Fe and specially HZ compared to Ni/Fe. This difference between Fe and Ni/Fe can be attributed to the presence of nickel particles on the Ni/Fe surface of biochar, acting as a heat-resistant metal and enhancing the thermal stability of the sample. Moreover, the DTG curve for HZ biochar shows a gradual weight loss starting from around 200 °C, contrasting with the other two samples. The weight losses in this temperature range, overlapping with the degradation of hemicelluloses, cellulose, and lignin [53], were 4.1%, 3.8%, and 9.6% for Fe, Ni/Fe, and HZ, respectively. These differences suggest the positive impact of metal catalysts in enhancing thermal resistance. The major weight loss peak for Fe (6.3%) and Ni/Fe (5.4%) biochars occurred in the range of 600-750 °C. This suggests that the resistance of nickel and iron metals to degradation diminishes at higher temperatures. HZ biochar showed a 7.1% weight loss in this range, closer to the other two samples compared to the previous temperature range. The overall weight losses for Fe, Ni/Fe, and HZ biochars were 15.16%, 14.75%, and 23.85%, respectively.

In a study by Pariyar et al. on biochar from pyrolysis of kitchen waste at 550 °C, which has relatively similar conditions and waste to this study, the weight loss was around 36% [54]. The difference in thermal stability between the biochars of the aforementioned and the present study could be attributed to the presence of catalysts on the biochar's surfaces in this research. Catalysts can reduce activation energy and enhance the decomposition of feedstock, leading to a better pyrolysis process [37]. Priya et al. also observed weight losses of around 17-30% for biochars pyrolyzed at 650 °C [54], closer to the results of this study, further supporting the impact of catalysts on enhancing the quality of the pyrolysis process.

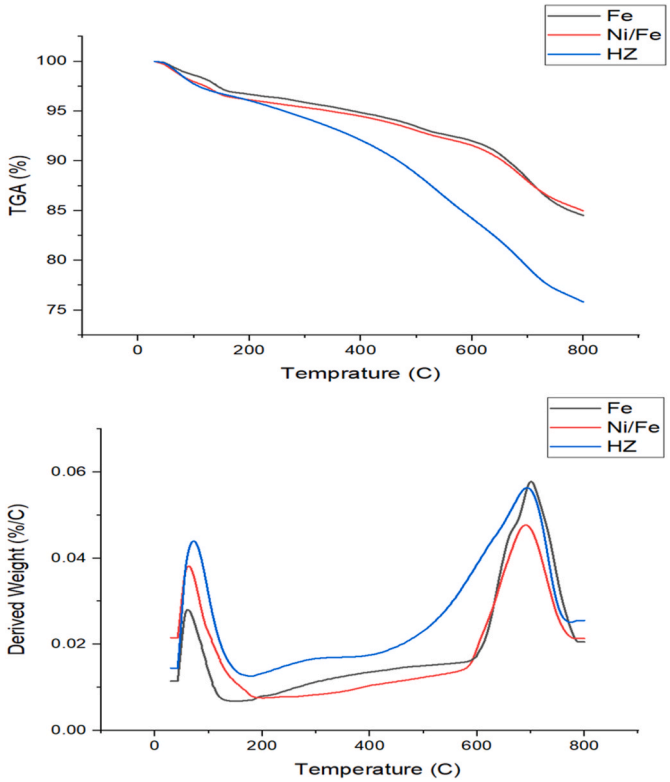

Fig. 5. TGA/DTG analysis, above) TGA, below) DTG.

The presence of catalysts, especially metal catalysts, on the surface of the biochar samples enhances their thermal stability, making them promising candidates for applications such as catalysis, energy storage, and electrodes, where biochars are exposed to high temperatures.

4. Conclusion

The findings of this study underscore the significance of catalyst selection in influencing product distribution and biochar properties from catalytic fast pyrolysis of household waste. The key novel contributions are: (1) systematic demonstration that catalyst chemistry (acidic zeolite vs. basic/neutral zeolite vs. redox-active metal oxide) fundamentally alters biochar yield, surface area, and thermal stability; (2) identification of Fe_3O_4 as a superior catalyst for producing high-surface-area biochar (480 m^2/g) without post-treatment; and (3) elucidation that Ni and Co coatings, while reducing surface area, significantly enhance thermal stability (up to ~15% weight loss), offering a trade-off for applications requiring thermal resistance.

Notably, HZSM-5-based catalysts demonstrated superior biochar yield, while Fe_3O_4-based catalysts exhibited higher bio-oil production. Moreover, the coating of catalysts with nickel and cobalt impacted product yields and biochar characteristics. It was observed that the use of transition metals reduced the bio-oil yield in favor of more biogas production. Also, despite reductions in specific surface area and porosity observed in coated catalyst samples, the presence of catalysts on biochar's surface presented opportunities for catalytic and energy storage applications, as they provide an abundant number of active sites on the surface of biochar. It is worth noting that using uncoated catalysts resulted in biochars with high surface areas compared to ordinary biochar of fast pyrolysis. Additionally, the presence of catalysts on the surface of biochars was seen to enhance their thermal stability due to their ability to promote pyrolysis reactions and the heat resistance of metal-containing catalysts, which further improved this quality.

Although these biochars have a higher surface area than most biochars produced from fast pyrolysis, without additional operations, they have relatively low surface area and porosity, which usually cannot meet the requirements of practical applications [27]. Therefore, it is necessary for these biochars to undergo a post-treatment process. Post-treatment methods such as activation (physical or chemical), ball milling, coating with carbonaceous materials, chemical modification, etc., can significantly improve the surface area and porosity of biochar.

A key limitation of this study is the lack of catalyst reusability, stability, and regeneration analysis; future work will investigate the recyclability of these catalysts and the long-term stability of the produced biochars. Additionally, the proposed applications in catalysis and energy storage were not experimentally demonstrated and remain speculative pending further characterization and performance testing. Future research could explore the specific catalytic activities of the produced biochars and their potential applications in various fields, including quantitative assessment of their performance in real-world applications such as soil amendment, wastewater treatment, or electrode materials. Additionally, optimizing the pyrolysis process parameters and catalyst characteristics, including variation of metal loading and systematic gas composition analysis, would provide deeper mechanistic insights.

CRediT authorship contribution statement

Alireza Namdar Zangeneh: Data curation, Formal analysis, Writing

– original draft. **Maryam Abbasi:** Investigation, Methodology, Supervision, Validation, Writing – review & editing. **Payam Ghorbannezhad:** Conceptualization, Project administration, Supervision, Validation, Visualization, Writing – review & editing.

Acknowledgement

The authors gratefully acknowledge Shahid Beheshti University (SBU), the National University of Iran, for financial support. Partial funding was provided by the Alexander von Humboldt Foundation (AvH), Germany. The Karlsruhe Institute of Technology (KIT), Germany, is acknowledged for providing laboratory facilities and technical resources, with special thanks to the IKFT technical staff for their valuable assistance.

Data availability

Data will be made available on request.

References

[1] B. Wang, Y. Fu, H. Zheng, D. Zeng, R. Xiao, Catalytic and noncatalytic fast pyrolysis of waste tires to produce high-value monocyclic aromatic hydrocarbons, J. Anal. Appl. Pyrolysis 156 (2021) 105131, https://doi.org/10.1016/j.jaap.2021.105131.
[2] S. Kaza, L. Yao, P. Bhada-Tata, F. Van Woerden, What a Waste 2.0: a Global Snapshot of Solid Waste Management to 2050, The World Bank, 2018, https://doi.org/10.1596/978-1-4648-1329-0.
[3] S. Saikia, A.S. Kalamdhad, Assessment of pyrolysis potential of Indian municipal solid waste and legacy waste via physicochemical and thermochemical characterization, Bioresour. Technol. 394 (2024) 130289, https://doi.org/10.1016/j.biortech.2023.130289.
[4] J. Ye, X. Chen, C. Chen, B. Bate, Emerging sustainable technologies for remediation of soils and groundwater in a municipal solid waste landfill site – A review, Chemosphere 227 (2019) 681–702, https://doi.org/10.1016/j.chemosphere.2019.04.053.
[5] P. Ghorbannezhad, N. Soleymani, M. Abbasi, Co-pyrolysis of municipal and horticultural wastes for enhanced biochar and bio-oil production: a response surface methodology approach, Fuel 350 (2023) 128795, https://doi.org/10.1016/j.fuel.2023.128795.
[6] B. Liu, Z. Han, X. Liang, Dioxin emissions from municipal solid waste incineration in the context of waste classification policy, Atmos. Pollut. Res. 14 (8) (2023) 101842, https://doi.org/10.1016/j.apr.2023.101842.
[7] T. Jia, F. Zhou, H. Ma, Y. Zhang, A highly stable waste animal bone-based catalyst for selective nitriles production from biomass via catalytic fast pyrolysis in NH3, J. Anal. Appl. Pyrolysis 157 (2021) 105217, https://doi.org/10.1016/j.jaap.2021.105217.
[8] R.K. Mishra, K. Mohanty, A review of the next-generation biochar production from waste biomass for material applications, Sci. Total Environ. 904 (2023) 167171, https://doi.org/10.1016/j.scitotenv.2023.167171.
[9] P. Danesh, P. Niaparast, P. Ghorbannezhad, I. Ali, Biochar Production: recent developments, applications, and challenges, Fuel 337 (2023) 126889, https://doi.org/10.1016/j.fuel.2022.126889.
[10] J. Luo, Q. Wang, L. Lin, S. Zhang, X. Zhu, Waste plastics complement biochar: innovative approach in curbing toxicants (KCN/NaCN) in N-Containing biochar, ACS Sustain. Chem. Eng. 9 (12) (2021) 4617–4624, https://doi.org/10.1021/acssuschemeng.1c00226.
[11] N. Cai, X. Li, S. Xia, L. Sun, J. Hu, P. Bartocci, F. Fantozzi, P. Williams, Y. Haiping, H. Chen, Pyrolysis-catalysis of different waste plastics over Fe/Al 2 O 3 catalyst: high-value hydrogen, liquid fuels, carbon nanotubes and possible reaction mechanisms, Energy Convers. Manag. 229 (2021) 113794, https://doi.org/10.1016/j.enconman.2020.113794.
[12] S. Srinivasan, A.S. Valsadwala, S. Shamshath Begum, A.B. Samui, Experimental investigation on the influence of novel catalyst in co-pyrolysis of polymeric waste: characterization of oil and preparation of char reinforced composites, J. Clean. Prod. 316 (2021) 128225, https://doi.org/10.1016/j.jclepro.2021.128225.
[13] S. Wang, Y. Sun, R. Shan, J. Gu, T. Huhe, X. Ling, H. Yuan, Y. Chen, Polypropylene pyrolysis and steam reforming over Fe-based catalyst supported on activated carbon for the production of hydrogen-rich syngas, Carbon Resour. Convers. 6 (3) (2023) 173–182, https://doi.org/10.1016/j.crcon.2023.02.004.
[14] S. Yousef, J. Eimontas, N. Striūgas, M.A. Abdelnaby, Synthesis of value-added aromatic chemicals from catalytic pyrolysis of waste wind turbine blades and their kinetic analysis using artificial neural network, J. Anal. Appl. Pyrolysis 177 (2024) 106330, https://doi.org/10.1016/j.jaap.2023.106330.
[15] C. Li, Y. Sun, S. Zhang, Y. Tang, D. Wang, X. Hu, Co-pyrolysis of waste paper and tyre: exploration of interaction of volatiles of varied origin and the influence on product evolution, J. Anal. Appl. Pyrolysis 178 (2024) 106395, https://doi.org/10.1016/j.jaap.2024.106395.
[16] A. Nawaz, S.A. Razzak, Co-pyrolysis of biomass and different plastic waste to reduce hazardous waste and subsequent production of energy products: a review on advancement, synergies, and future prospects, Renew. Energy 224 (2024) 120103, https://doi.org/10.1016/j.renene.2024.120103.
[17] D. Singh, A. Paul, Characterization and performance evaluation of co-pyrolysis oil from waste cooking oil and waste polyethylene as a potential diesel substitute, Fuel 362 (2024) 130739, https://doi.org/10.1016/j.fuel.2023.130739.
[18] P. Li, X. Shi, X. Wang, J. Song, S. Fang, J. Bai, G. Zhang, C. Chang, S. Pang, Bio-oil from biomass fast pyrolysis: yields, related properties and energy consumption analysis of the pyrolysis system, J. Clean. Prod. 328 (2021) 129613, https://doi.org/10.1016/j.jclepro.2021.129613.
[19] D. Zhang, Y. Zhang, H. Liu, Y. Xu, J. Wu, P. Li, Effect of pyrolysis temperature on carbon materials derived from reed residue waste biomass for use in supercapacitor electrodes, J. Phys. Chem. Solid. 178 (2023) 111318, https://doi.org/10.1016/j.jpcs.2023.111318.
[20] H. Jiang, C. Yang, J. Song, Y. Li, W. Jia, M. Song, Conversion of waste mask into hydrocarbon-rich fuels through catalytic pyrolysis with Zr-Mg metal-adopted catalyst under N2/CO2 atmosphere, J. Anal. Appl. Pyrolysis 178 (2024) 106410, https://doi.org/10.1016/j.jaap.2024.106410.
[21] P. Premchand, F. Demichelis, D. Chiaramonti, S. Bensaid, D. Fino, Study on the effects of carbon dioxide atmosphere on the production of biochar derived from slow pyrolysis of organic agro-urban waste, Waste Manag. 172 (2023) 308–319, https://doi.org/10.1016/j.wasman.2023.10.035.
[22] Q. Wu, W. Huang, A. Dai, L. Ke, L. Zhang, Q. Zhang, X. Cui, L. Fan, C. Xu, K. Cobb, R. Zou, X. Pan, Y. Liu, R. Ruan, Y. Wang, Two-step fast pyrolysis of torrefied corncobs and waste cooking oil under different atmosphere for hydrocarbons production, Energy 286 (2024) 129535, https://doi.org/10.1016/j.energy.2023.129535.
[23] J.G. Hwang, B.K. Lee, M.K. Choi, H.C. Park, H.S. Choi, Optimal production of waste tire pyrolysis oil and recovery of high value-added D-limonene in a conical spouted bed reactor, Energy 262 (2023) 125519, https://doi.org/10.1016/j.energy.2022.125519.
[24] Y. Li, Y. Zhang, K. Qian, W. Huang, Metal–Support interactions in Metal/Oxide catalysts and oxide–metal interactions in Oxide/Metal inverse catalysts, ACS Catal. 12 (2) (2022) 1268–1287, https://doi.org/10.1021/acscatal.1c04854.
[25] K. Li, Y. Wang, W. Zhou, T. Cui, J. Yang, Z. Sun, Y. Min, J.M. Lee, Catalytic pyrolysis of film waste over Co/Ni pillared montmorillonites towards H(2) production, Chemosphere 299 (2022) 134440, https://doi.org/10.1016/j.chemosphere.2022.134440.
[26] K. Wang, T. Shan, B. Li, Y. Zheng, H. Xu, C. Wang, X. Tian, Study on pyrolysis characteristics, kinetics and thermodynamics of waste tires catalytic pyrolysis with low-cost catalysts, Fuel 356 (2024) 129644, https://doi.org/10.1016/j.fuel.2023.129644.
[27] L. Leng, Q. Xiong, L. Yang, H. Li, Y. Zhou, W. Zhang, S. Jiang, H. Li, H. Huang, An overview on engineering the surface area and porosity of biochar, Sci. Total Environ. 763 (2021) 144204, https://doi.org/10.1016/j.scitotenv.2020.144204.
[28] J. Raček, T. Chorazy, M.C. Miino, M. Vršanská, M. Brtnický, L. Mravcová, J. Kučerík, P. Hlavínek, Biochar production from the pyrolysis of food waste: characterization and implications for its use, Sustain. Chem. Pharm. 37 (2024) 101387, https://doi.org/10.1016/j.scp.2023.101387.
[29] M. Abbasi, N. Rastgoo, B. Nakisa, Monthly and seasonal modeling of municipal waste generation using radial basis function neural network, Environ. Prog. Sustain. Energy 38 (2018), https://doi.org/10.1002/ep.13033.
[30] N. Miskolczi, N. Gao, C. Quan, Pyrolysis-gasification of biomass and Municipal Plastic Waste using transition metal modified catalyst to investigate the effect of contaminants, J. Energy Inst. 108 (2023) 101233, https://doi.org/10.1016/j.joei.2023.101233.
[31] M.A.A. Mohamad Dzol, V. Balasundram, K. Shameli, N. Ibrahim, Z.A. Manan, R. Isha, Catalytic pyrolysis of high-density polyethylene over nickel-waste chicken eggshell/HZSM-5, J. Environ. Manag. 324 (2022) 116392, https://doi.org/10.1016/j.jenvman.2022.116392.
[32] A. Tomczyk, Z. Sokołowska, P. Boguta, Biochar physicochemical properties: pyrolysis temperature and feedstock kind effects, Rev. Environ. Sci. Biotechnol. 19 (2020), https://doi.org/10.1007/s11157-020-09523-3.
[33] L. Leng, H. Huang, An overview of the effect of pyrolysis process parameters on biochar stability, Bioresour. Technol. 270 (2018) 627–642, https://doi.org/10.1016/j.biortech.2018.09.030.
[34] Y. Li, R. Gupta, Q. Zhang, S. You, Review of biochar production via crop residue pyrolysis: development and perspectives, Bioresour. Technol. 369 (2023) 128423, https://doi.org/10.1016/j.biortech.2022.128423.
[35] J.A. Allen, A.E. Downie, Predicting slow pyrolysis process outcomes with simplified empirical correlations for a consistent higher heating temperature: biochar yield and ash content, Energy & Fuels 34 (11) (2020) 14223–14231, https://doi.org/10.1021/acs.energyfuels.0c02597.
[36] B.T. Nguyen, J. Lehmann, W.C. Hockaday, S. Joseph, C.A. Masiello, Temperature sensitivity of Black carbon decomposition and oxidation, Environ. Sci. Technol. 44 (9) (2010) 3324–3331, https://doi.org/10.1021/es903016y.
[37] A.T. Sipra, N. Gao, H. Sarwar, Municipal solid waste (MSW) pyrolysis for bio-fuel production: a review of effects of MSW components and catalysts, Fuel Process. Technol. 175 (2018) 131–147, https://doi.org/10.1016/j.fuproc.2018.02.012.
[38] P. Ghorbannezhad, S. Park, J.A. Onwudili, Co-pyrolysis of biomass and plastic waste over zeolite- and sodium-based catalysts for enhanced yields of hydrocarbon products, Waste Manag. 102 (2020) 909–918, https://doi.org/10.1016/j.wasman.2019.12.006.
[39] N. Priharto, S. Ghysels, M. Pala, W. Opsomer, F. Ronsse, G. Yildiz, H.J. Heeres, P. J. Deuss, W. Prins, Ex situ catalytic fast pyrolysis of lignin-rich digested stillage over Na/ZSM-5, H/ZSM-5, and Fe/ZSM-5, Energy & Fuels 34 (10) (2020) 12710–12723, https://doi.org/10.1021/acs.energyfuels.0c02390.

[40] Q. Liu, J. Wang, J. Zhou, Z. Yu, K. Wang, Promotion of monocyclic aromatics by catalytic fast pyrolysis of biomass with modified HZSM-5, J. Anal. Appl. Pyrolysis 153 (2021) 104964, https://doi.org/10.1016/j.jaap.2020.104964.
[41] M. Jouiad, N. Al-Nofeli, N. Khalifa, F. Benyettou, L.F. Yousef, Characteristics of slow pyrolysis biochars produced from rhodes grass and fronds of edible date palm, J. Anal. Appl. Pyrolysis 111 (2015) 183–190, https://doi.org/10.1016/j.jaap.2014.10.024.
[42] A. El-Naggar, S.M. Shaheen, S.X. Chang, D. Hou, Y.S. Ok, J. Rinklebe, Biochar surface functionality plays a vital role in (Im)Mobilization and phytoavailability of soil vanadium, ACS Sustain. Chem. Eng. 9 (19) (2021) 6864–6874, https://doi.org/10.1021/acssuschemeng.1c01656.
[43] R. French, S. Czernik, Catalytic pyrolysis of biomass for biofuels production, Fuel Process. Technol. 91 (1) (2010) 25–32, https://doi.org/10.1016/j.fuproc.2009.08.011.
[44] A. Ochoa, J. Bilbao, A.G. Gayubo, P. Castaño, Coke formation and deactivation during catalytic reforming of biomass and waste pyrolysis products: a review, Renew. Sustain. Energy Rev. 119 (2020) 109600, https://doi.org/10.1016/j.rser.2019.109600.
[45] N.S. Kumar, H.M. Shaikh, M. Asif, E.H. Al-Ghurabi, Engineered biochar from wood apple shell waste for high-efficient removal of toxic phenolic compounds in wastewater, Sci. Rep. 11 (1) (2021) 2586, https://doi.org/10.1038/s41598-021-82277-2.
[46] T. Rout, D. Pradhan, R.K. Singh, N. Kumari, Exhaustive study of products obtained from coconut shell pyrolysis, J. Environ. Chem. Eng. 4 (3) (2016) 3696–3705, https://doi.org/10.1016/j.jece.2016.02.024.
[47] A. Shaaban, S.-M. Se, N.M.M. Mitan, M.F. Dimin, Characterization of biochar derived from rubber wood sawdust through slow pyrolysis on surface porosities and functional groups, Procedia Eng. 68 (2013) 365–371, https://doi.org/10.1016/j.proeng.2013.12.193.
[48] D.P. Serrano, J.A. Melero, G. Morales, J. Iglesias, P. Pizarro, Progress in the design of zeolite catalysts for biomass conversion into biofuels and bio-based chemicals, Catal. Rev. 60 (1) (2018) 1–70, https://doi.org/10.1080/01614940.2017.1389109.
[49] Y. Shen, P. Zhao, Q. Shao, D. Ma, F. Takahashi, K. Yoshikawa, In-situ catalytic conversion of tar using rice husk char-supported nickel-iron catalysts for biomass pyrolysis/gasification, Appl. Catal. B Environ. 152–153 (2014) 140–151, https://doi.org/10.1016/j.apcatb.2014.01.032.
[50] M.J. Antal, M. Grønli, The art, science, and technology of charcoal production, Ind. Eng. Chem. Res. 42 (8) (2003) 1619–1640, https://doi.org/10.1021/ie0207919.
[51] K. Weber, P. Quicker, Properties of biochar, Fuel 217 (2018) 240–261, https://doi.org/10.1016/j.fuel.2017.12.054.
[52] J.L. Santos, P. Mäki-Arvela, A. Monzón, D.Y. Murzin, M.Á. Centeno, Metal catalysts supported on biochars: part I synthesis and characterization, Appl. Catal. B Environ. 268 (2020) 118423, https://doi.org/10.1016/j.apcatb.2019.118423.
[53] B.B. Uzun, A.E. Pütün, E. Pütün, Composition of products obtained via fast pyrolysis of olive-oil residue: effect of pyrolysis temperature, J. Anal. Appl. Pyrolysis 79 (1) (2007) 147–153, https://doi.org/10.1016/j.jaap.2006.12.005.
[54] P. Pariyar, K. Kumari, M.K. Jain, P.S. Jadhao, Evaluation of change in biochar properties derived from different feedstock and pyrolysis temperature for environmental and agricultural application, Sci. Total Environ. 713 (2020) 136433, https://doi.org/10.1016/j.scitotenv.2019.136433.